Light scattering from WDM filters

Michel Lequime, Carole Deumié and Claude Amra*

Laboratoire d'Optique des Surfaces et des Couches Minces – UPRES A CNRS 6080
Ecole Nationale Supérieure de Physique de Marseille 13397 Marseille Cedex 20 – France

ABSTRACT

Light scattering is well known to be a key limitation of the ultimate performances of filters. Whatever the values of surface roughness and bulk heterogeneity within the multilayer, the optical losses depend on the stack design and on the correlation factors between defects. Such situation is largely enhanced in the case of WDM filters, due to the high over-intensity of the electric field within the stack, as a consequence of the narrow pass-band. In this paper, we present some experimental scattering results recorded with an high angular and spectral resolution on prototype WDM filters and which illustrate the enhancement of scattering near the design wavelength of the filter.

Keywords : fiber optic telecommunications, WDM components, narrow band-pass filters, thin film multilayers, scattering

1. INTRODUCTION

It is clear that the quick development of fiber optic telecommunication networks is closely connected to the recent availability of some critical items, like :

- low loss and high bandwidth single mode fibers, whose zero dispersion wavelength has been shifted around 1550 nanometers, the spectral window corresponding to the minimum of attenuation of silica fibers,
- narrow linewidth semiconductor lasers, Distributed Feedback (DFB) type, with low noise figure and thermal tuning ability on a small spectral range,
- powerful optical amplifiers, based on the use of Erbium doped fibers or semiconductor lasers, which allow the efficient regeneration of several optical signals in parallel into a single monomode fiber,
- Wavelength Division Multiplexing (WDM) components, which made possible some important routing functions into a multi-wavelength fiber optic network.

WDM components appear really as one of the most important items of this technical evolution, and different kinds of solutions (Fiber Bragg Gratings reflectors, Optical Guided Wave filters and Optical Interference Coatings) are still in competition to satisfy the always more stringent requirements of the telecommunications industry : decrease of the bandwidth (channel spacing of 400 GHz, recently lowered to 200 GHz and the evolution towards 100 GHz is now under study), reduction of the insertion losses, increase of the isolation factor,… We have chosen to participate to the development of WDM components based on the use of optical interference coatings, in which the know-how of our laboratory is important and covers all the aspects of this problem, i.e. design, modeling, manufacturing and characterization.

The objectives of this paper are first to recall some general results on the theoretical description of the scattering phenomena in such narrow-band pass filters, secondly to describe the experimental set-up that we have developed to perform the complete characterization of the scattering properties of WDM filters and last to provide with some experimental results that we have obtained with it on two prototype filters.

2. THEORETICAL ANALYSIS

Theoretical tools have been investigated in the LOSCM to predict and analyze light scattering effects from optical coatings. A first-order vector permits to predict surface or bulk scattering. These models do not access to cross-polarized light in the incidence plane. They have been largely published and confirmed by experiment [1-3].

* For further author information :
M.L. : Email michel.lequime@enspm.u-3mrs.fr ; Telephone (+33) 4 91 28 83 95 ; Fax (+33) 4 91 28 80 67
C.D. : Email carole.deumié@enspm.u-3mrs.fr ; Telephone (+33) 4 91 28 83 92 ; Fax (+33) 4 91 28 80 67
C.A. : Email claude.amra@enspm.u-3mrs.fr ; Telephone (+33) 4 91 28 80 70 ; Fax (+33) 4 91 28 80 67

In the case of the surface model, height irregularities at interfaces are assumed to be much less than the illumination wavelength :

$$\left| h(\vec{r})/\lambda \right| << 1$$

where $h(\vec{r}) = h(x,y)$ is the interface profile and λ is the incident wavelength. Such an hypothesis is largely justified for optical wavelengths and polished substrates.

In the case of the bulk model, the relative variations in the layer permittivity are assumed to be much less than unity :

$$\left| \Delta\varepsilon \ /\varepsilon \right| = p(\vec{r},z) \ << \ 1$$

Such an hypothesis is largely justified except if scattering originates from some particular localized defects with a strong discontinuity in the refractive index.

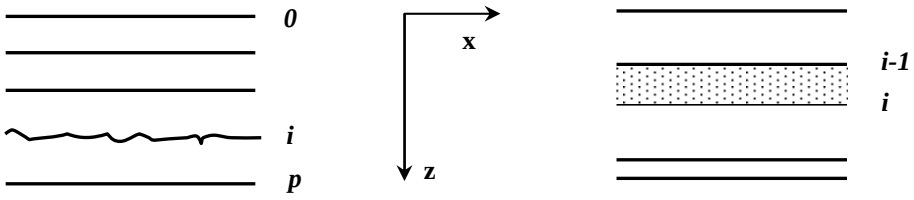

(a) Interface roughness *(b) Bulk inhomogeneity*

Figure 1

The Figure 1 shows a schematic view of interface roughness (*a*) and bulk inhomogeneity (*b*) inside a multilayer stack, the medium (*i*) being located between the interfaces (*i-1*) and (*i*), where *0* is the incident air medium.

The scattered intensity I in the direction (θ, ϕ) of space, where θ is the scattering angle and ϕ the polar angle, is given by :

$$I(\theta,\phi) = \sum_{i,j} C_{ij} \ \alpha_{ij} \ \gamma_{jj}$$

where C_{ij} is an optical factor depending on the multilayer formula, the illumination and observation conditions, γ_{jj} is the roughness or permittivity spectrum, depending on bulk or surface effects, while α_{ij} describes the correlation between (*i*) and (*j*) surfaces or between (*i*) and (*j*) bulks.

In the case of surface scattering, γ_{jj} is the roughness spectrum of the (*j*) interface :

$$\gamma_{jj} = \frac{4\pi^2}{S} \left| \hat{h}_j(\vec{\sigma}) \right|^2$$

where S is the surface, $\vec{\sigma}/2\pi = (\sin\theta/\lambda)\{\cos\phi;\sin\phi\}$ is the spatial frequency (θ is the scattering angle from the sample normal and ϕ the polar angle), $\hat{h}_j$ the Fourier transform of the interface (*j*) profile. The roughness δ, or root mean square, is defined as :

$$\delta_j{}^2 = \frac{1}{S}\int_S h_j{}^2(\vec{r})\,d\vec{r} = \int_{\vec{\sigma}} \gamma_{jj}(\vec{\sigma})\,d\vec{\sigma}$$

with $d\vec{r} = dx\,dy$ and $d\vec{\sigma} = d\sigma_x\ d\sigma_y$.

In the case of bulk scattering, γ_{jj} is the permittivity spectrum :

$$\gamma_{jj} = \frac{4\pi^2}{S} \left| \hat{p}_j(\vec{\sigma}) \right|^2$$

where $\hat{p}_j(\vec{\sigma})$ is the Fourier transform of the permittivity relative variation of the (*j*) layer.

The normalized root mean square or relative inhomogeneity in the refractive index is given as

$$\left(\frac{\delta_j}{n_j}\right)^2 = \left(\frac{\Delta n_j}{n_j}\right)^2 = \frac{1}{4}\int_{\vec{\sigma}} \gamma_{jj}(\vec{\sigma})\, d\vec{\sigma}$$

As for numerical calculation, the spectra will be taken as isotropic functions given by the Fourier transform of the sum of a Gaussian and an exponential :

$$\gamma_{jj}(\sigma) = FT\left\{ {\delta_g}^2 e^{-\left(\frac{\tau}{L_g}\right)^2} + {\delta_e}^2 e^{-\frac{\tau}{L_e}} \right\}$$

$$\gamma_{jj}(\sigma) = \frac{1}{4\pi}(\delta_g L_g)^2 e^{-\left(\frac{\sigma L_g}{2}\right)^2} + \frac{1}{2\pi}\frac{(\delta_e L_e)^2}{\left[\sqrt{1+(\sigma L_e)^2}\right]^3}$$

In order to simulate surface or bulk scattering from WDM samples, we have to choose the δ_e , L_e , δ_g and L_g parameters, depending on the illumination wavelength. As shown in Figure 2, the angular behaviors of surface and bulk scattering are quite similar at normal illumination with the parameters :

$$\left.\begin{array}{l} \delta_e = 10\,\text{nm} \quad L_e = 2000\,\text{nm} \\ \delta_g = 0.5\,\text{nm} \quad L_g = 200\,\text{nm} \end{array}\right\} \text{for the surface spectrum}$$

$$\left.\begin{array}{l} \delta_e = 0.0007\,\text{nm} \quad L_e = 2000\,\text{nm} \\ \delta_g = 0.0004\,\text{nm} \quad L_g = 200\,\text{nm} \end{array}\right\} \text{for the bulk spectrum}$$

With these parameters, the interface roughness is δ = 1.12 nm and the bulk inhomogeneity is $\Delta n/n = 7.7\ 10^{-4}$. The illumination wavelength is λ = 1550 nm.

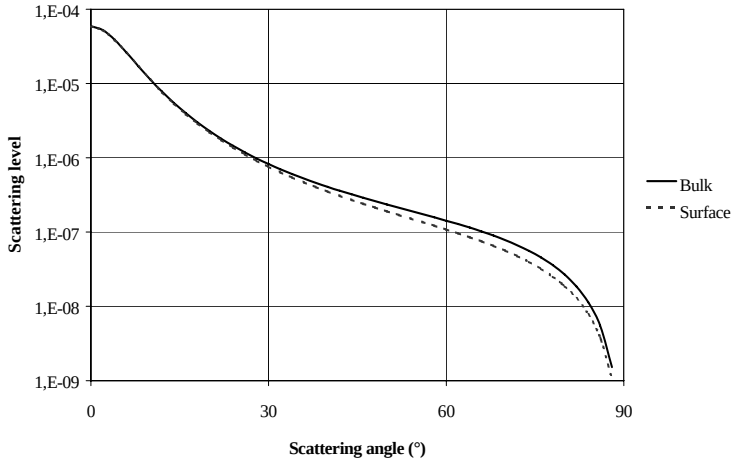

Figure 2

With these structural parameters we can simulate surface and bulk scattering in the case of multilayer components as Fabry-Perot filters. The Figure 3 shows the result of the simulation of angular bulk scattering in the case of a Fabry-Perot filter deposited on a glass substrate (design M18, 12H, M18 ; materials used Ta_2O_5/SiO_2) and illuminated at normal incidence and λ = 1.55 μm.

The Figure 4 shows the result of the simulation of angular surface scattering produced by the same component as above, the calculations being made for the case of correlated (subscript *Corr*) and uncorrelated (subscript *Uncorr*) surfaces.

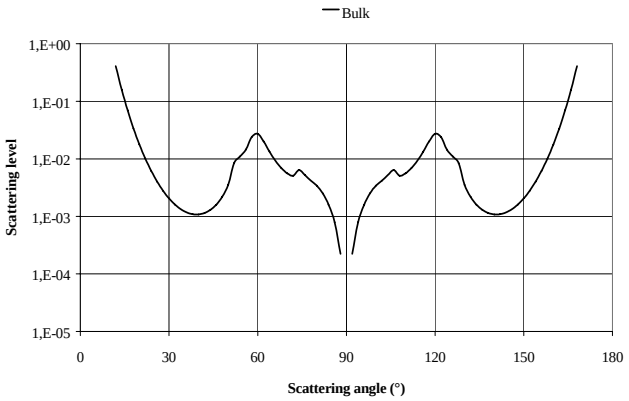

Figure 3

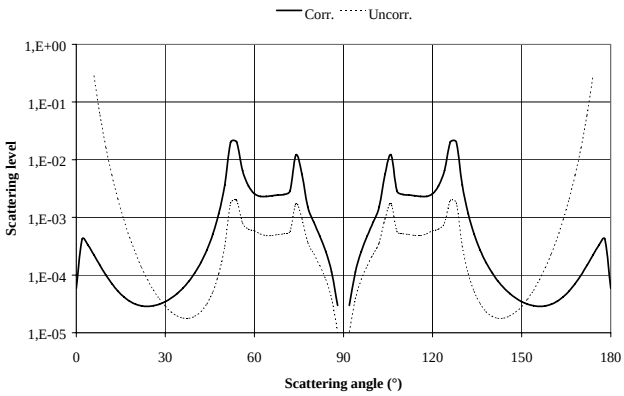

Figure 4

Experimental results on these type of optical multilayers are well known. They have shown that the scattering levels can not be explained thanks to a bulk effect. Moreover surface scattering originates from a correlated surfaces effect. In this case, we can reveal polarization influence, as shown in Figure 5, where SS is the subscript used for S incident polarization and S scattering polarization, while PP is the subscript used for P incident polarization and P scattering polarization.

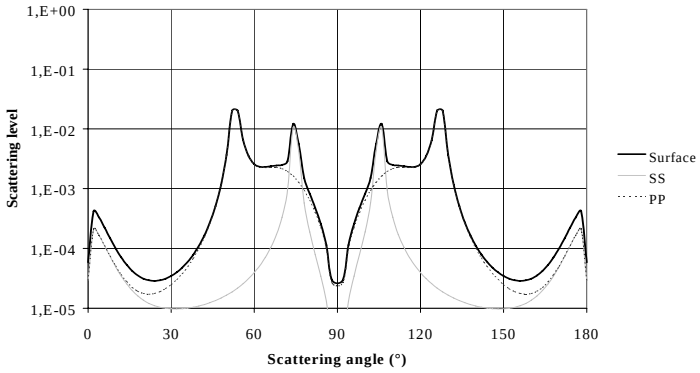

Figure 5

After these first results we can simulate light scattering from more complicated multilayers composed with the superposition of two Fabry-Perot filters. The result is a better rejection for WDM applications. We have shown in Figures 6 and 7 the results of such calculations in the case of bulk scattering (Figure 6) or correlated surfaces scattering (Figure 7) for a filter whose main characteristics are the following : design [M18, 12H, M18] B [M18, 12H, M18] ; materials used Ta_2O_5/SiO_2 ; illumination at normal incidence ; wavelength 1.55 µm.

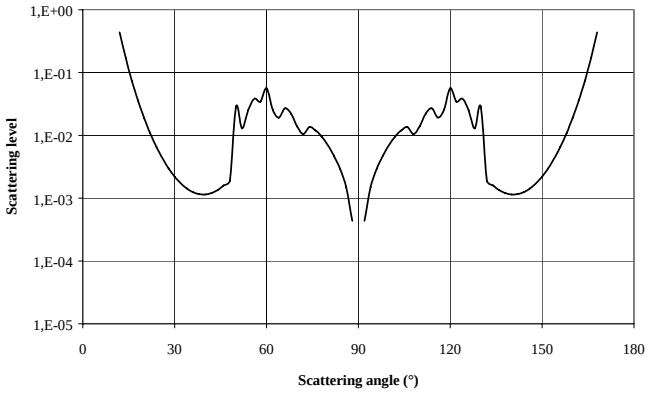

Figure 6

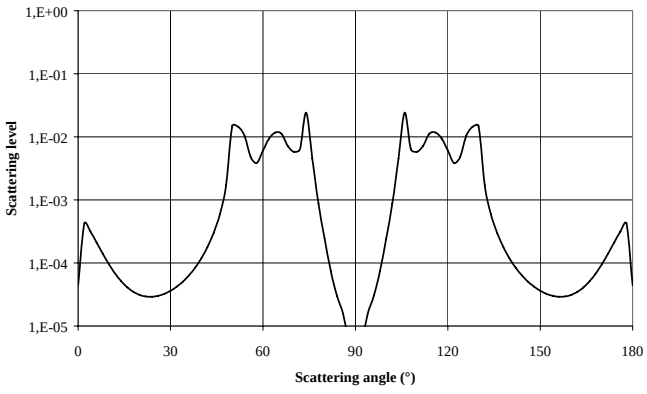

Figure 7

These results are in better agreement with experimental measurements (see section 4) in the case of the surface model. The Figure 8 shows moreover the influence of the state of polarization on these scattering rings, the choice of a linear scale allowing to better visualize their relative amplitude as well as their angular structure.

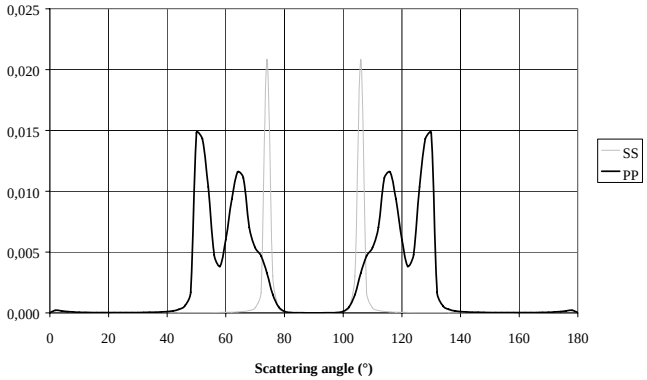

Figure 8

3. EXPERIMENTAL SET-UP

In order to characterize with a high angular and spectral resolution the scattering properties of such WDM filters around 1550 nanometers, we have developed a dedicated scattering measurement set-up which includes mainly (see Figure 9) :

- a tunable laser manufactured by EXFO (FLS-2600) around an Erbium doped fiber, and which produces about 2 mW CW into a line width of 10 picometer on the whole tuning range (1520 – 1570 nm). An important feature of this kind of tunable source is the spectral purity of the laser emission (side mode suppression ratio better than 65 dB), which allows to obtain very accurate spectral transmission data without any kind of extra filtering device. The wavelength resolution of the tuning is about 0.01 nm, while the tuning speed can be adjusted between 0.1 nm/s and 2.5 nm/s.
- a high dynamic range InGaAs detector, also manufactured by EXFO (IQ-1103), and which allows to detect light levels from 9 dBm to –90 dBm at a sampling rate of 5 Hz.

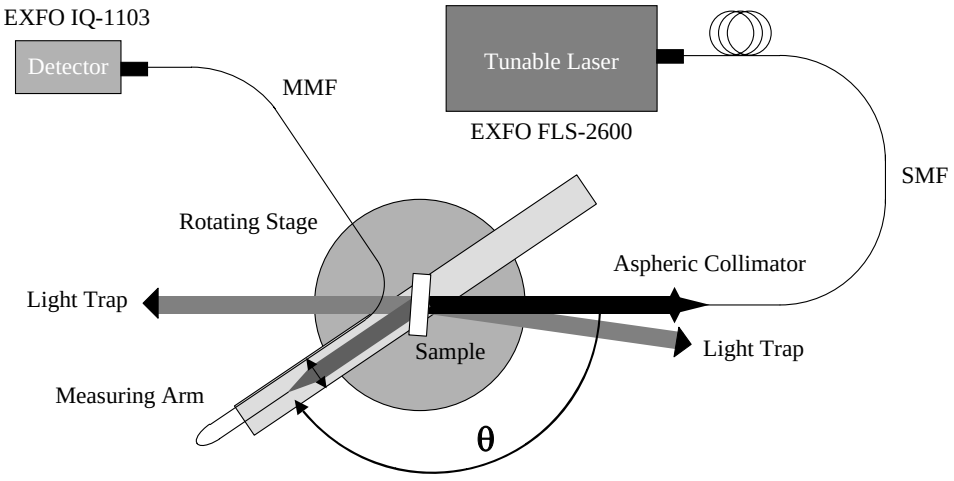

Figure 9

The light provided by the tunable laser is launched into a singlemode fiber whose output extremity is placed a the focal plane of a small aspheric lens, in order to illuminate the sample at 1.5° of incidence with a high quality collimated optical beam.

Two light traps are used to decrease the possible parasitic influence of the reflected and transmitted beams on our low level scattering measurements. The measuring arm includes also a multimode optical fiber located at the focal plane of a high quality lens, in order to reduce the optical throughput of the detection beam to the minimum requested value and decrease again the amount of parasitic light. The angular position of this detection arm can be changed with the help of a high accuracy rotating stage, whose angular displacement rate is about 0.35°/s. As a consequence, the angular resolution of our set-up is about 0.07°, while the spectral resolution is about 0.01nm, these two features being in accordance with the high performances required by the fine characterization of the scattering properties of WDM filters.

Finally, it shall be noticed that the combined use of a rotating stage for the measuring arm and of a detector with a very large dynamic range allows to record the spectral transmittance of the filter with the same illumination and observation conditions as used for the scattering measurements (especially the angle of incidence, but also the divergence and the transverse dimensions of the illuminated area at the sample surface).

4. RESULTS

We have used this dedicated experimental set-up to study the scattering properties of two prototype WDM filters available in our laboratory.

The first one (called Filter A) has the following performances (see Figures 10 and 11) :

Center wavelength : 1539.0 nm
Peak transmittance : 0.92
Bandwidth FWHM : 0.8 nm
Rejection factor : better than –45 dB

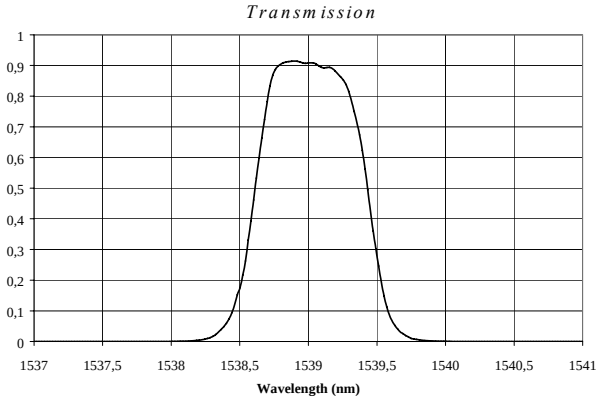

Figure 10

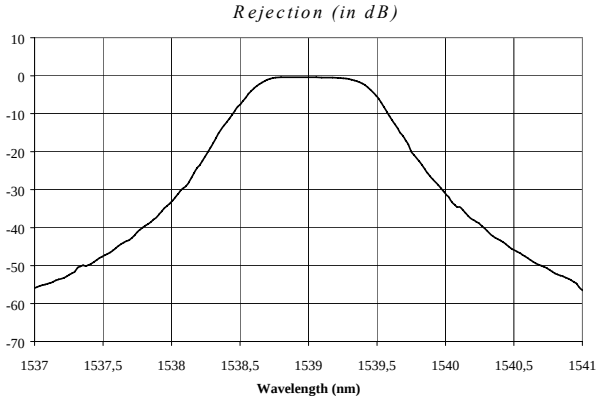

Figure 11

The Bi-directional Reflectance Distribution Function (BRDF) of this filter has been measured between 10° and 175°, in a in-plane configuration (polar angle equal to zero), and for various wavelengths comprised between 1537 and 1541 nm. Two typical examples are done in Figures 12 (log scale) and 13 (linear scale), and illustrate the fast decreasing of the amplitude of the scattering rings when the probe wavelength is slightly detuned from the central wavelength of the WDM filter.

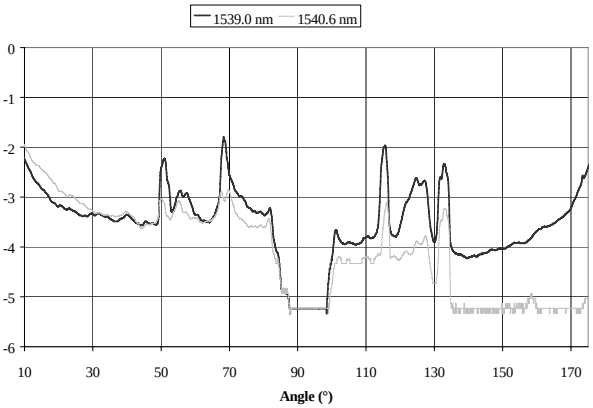

Figure 12

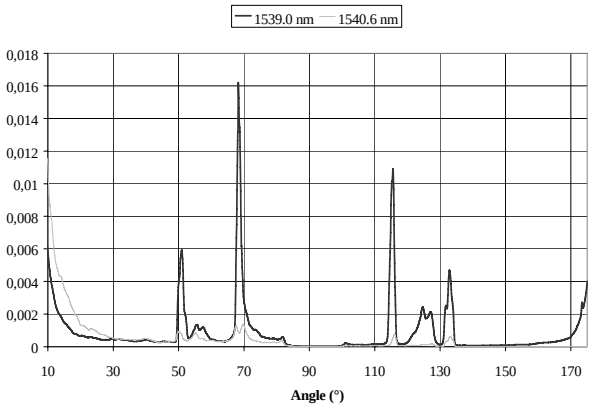

Figure 13

To summarize all the data recorded for the angular and spectral characterization of the scattering properties of such a filter, a possible way is to create a 2D representation, where the horizontal axis corresponds to the scattering angle θ and the vertical one to the wavelength λ, and where the value of the BRDF recorded for a given set (θ, λ) is represented by a dot whose brightness is chosen in accordance with a predefined gray scale. The Figure 14 shows the result obtained for the Filter A by using a gray level coded log scale.

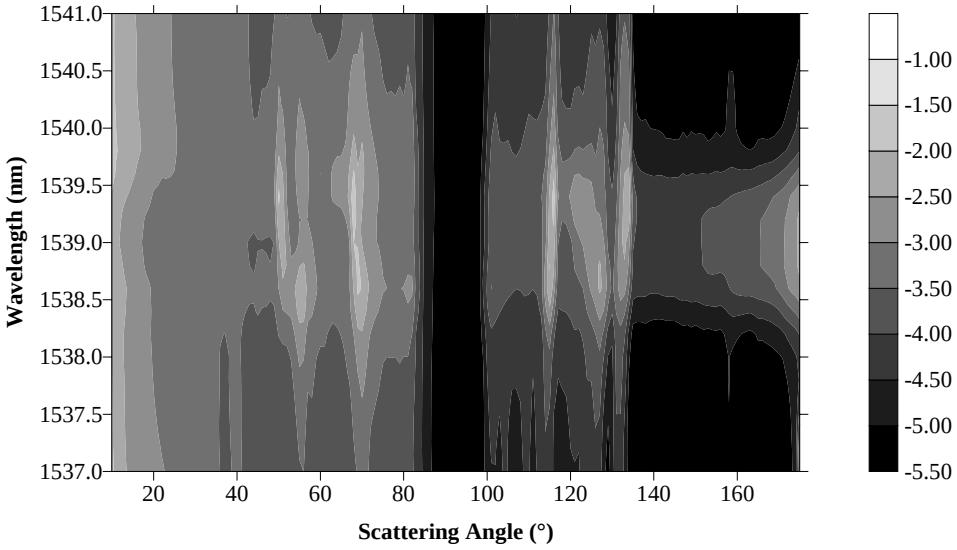

Figure 14

In such a graph, we can mainly notice :

- the presence of three sharp rings in the backward part of the scattered light (around 50°, 56° and 70°), whose intensity varies quickly with the wavelength and whose spectral dependence is characterized either by a single maximum (50° and 56°) or by two peaks separated by a low deep valley (70°) ; all these maximums are located apart from the central wavelength of the filter, the spectral detuning being about 0.5 nm.
- the small angular shifts of these rings with respect to the wavelength,
- the presence of three symmetrical rings in the forward part of the scattered light, whose shape is identical to the previous one, but whose intensity is slightly smaller.

Another way to summarize the scattering properties of such a filter is to represent the variations of the Total Integrated Scattering (TIS) factor (the backward one, the forward one and the sum of both) with respect to the wavelength, as see in Figure 15.

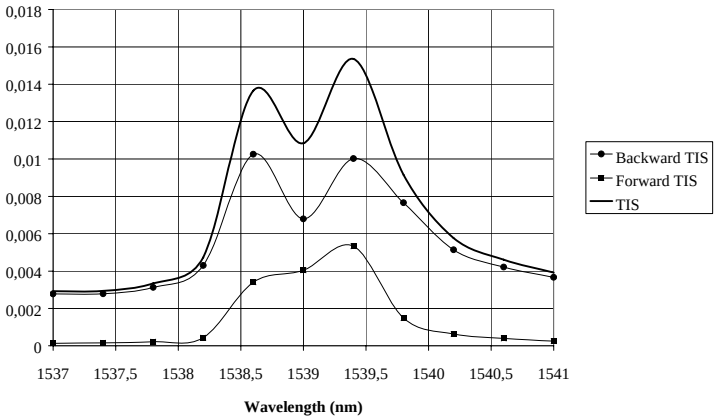

Figure 15

We find again the double peak behavior underlined above, as well as the decreasing of the scattering intensity in the forward regime with respect to the backward one. It means that the sharp rings structure includes the main part of the light scattered by such a filter.

The same kind of measurements have been performed in the case of a second prototype filter, named B. Its main performances are summarized hereafter (see Figures 16 and 17) :

Center wavelength : 1544.3 nm
Peak transmittance : 0.53

Bandwidth FWHM : 0.55 nm
Rejection factor : better than –30 dB

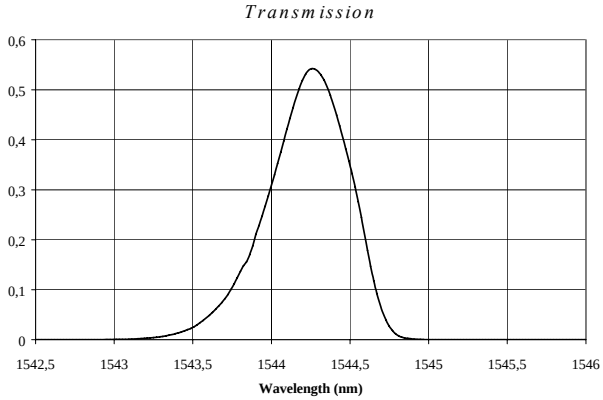

Figure 16

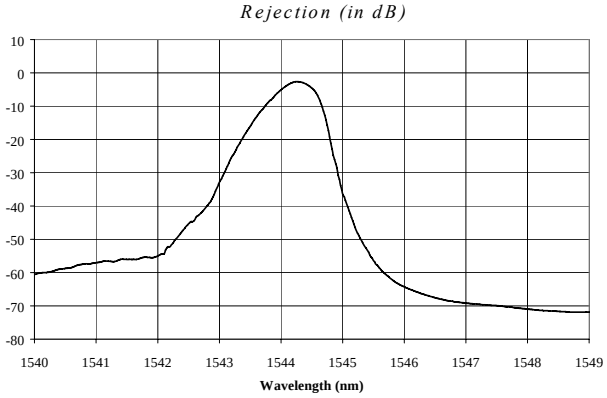

Figure 17

Even if its FWHM bandwidth is smaller (.55 nm instead of .8), the spectral performances of this filter B are in a general way poorer than their of the Filter A (lower peak transmittance, non symmetrical and triangular shape, smaller rejection ratio). The BRDF of this second filter has been measured in the same conditions as before (scattering angle comprised between 10° and 175°, in-plane configuration), and for a wavelength range from 1542.3 nm to 1546.1 nm. The Figure 18 summarizes all the recorded data, in the gray level graph mode defined above in the case of the filter A.

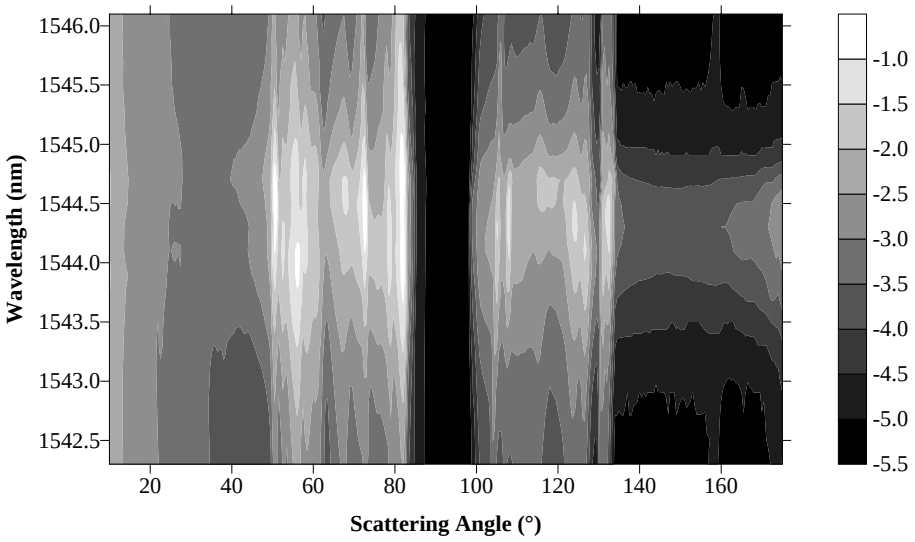

Figure 18

For this second filter, the number of angular resolved sharp rings is more important (7 instead of 3 in the backward scattering regime and naturally the same number in the forward regime, in symmetrical positions), and their contrast with respect to the scattered bottom is also more important as shown in the Figure 19 (probe wavelength equal to the central wavelength of the filter). By adding a polarizer to the illumination beam (direction of polarization S or P) and an analyzer to the measuring arm (direction of polarization S or P), we are able to study the influence of the state of polarization on the intensity of these scattering rings.

As shown in the Figure 20, the three rings which correspond to the higher scattering angles are associated to the SS configuration, and this result is in accordance with the prediction of our theoretical analysis (see Figure 8 for instance).

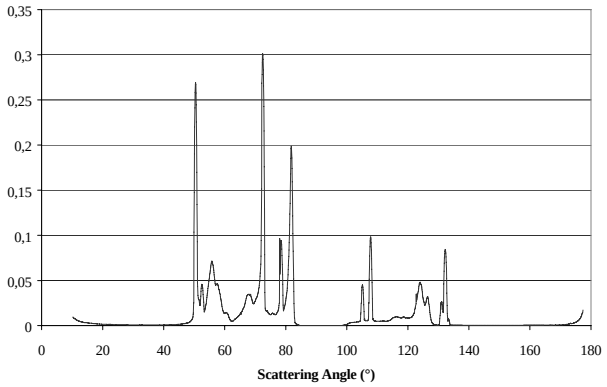

Figure 19

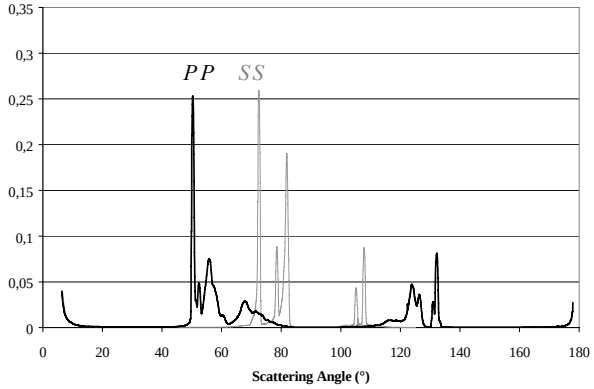

Figure 20

As previously used for the Filter A, it is possible to summarize the scattering properties of such a filter by representing the variations of the TIS factors with respect to the wavelength (Figure 21).

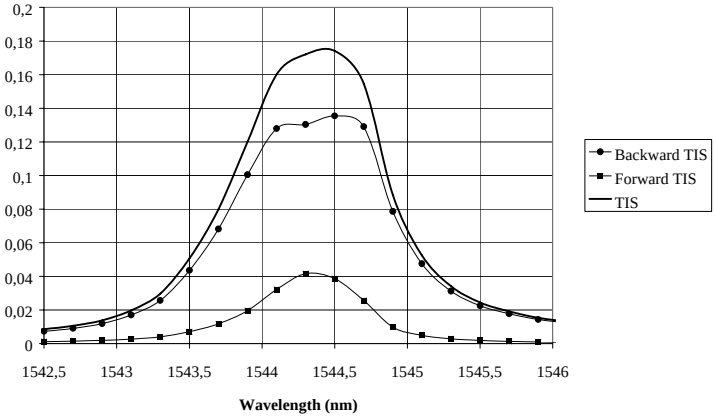

Figure 21

We can notice in this case the single peak behavior and the very high value of the TIS factor (about 20%), which is mainly due to the backward scattering regime.

5. CONCLUSIONS

High resolution angular and spectral BRDF measurements performed on prototype WDM filters have allowed to better understand the scattering phenomena in such narrow band-pass filters. Insertion losses are partly induced by the great amount of light scattered at high angles through ring shaped structures.

The occurrence of such enhancement phenomena shall be taken into account to optimize the design and the manufacturing of high performance WDM filters.

6. ACKNOWLEDGEMENTS

We would acknowledge MB Electronique and EXFO Europe for providing the tunable laser source FLS-2600 and the power meter IQ-1103, that we have used for our experimental characterizations.

7. REFERENCES

1. C. Amra, "*First order vector theory of bulk scattering in optical multilayers*", J. of the Opt. Soc. Of America A **10**, 365-374 (1993)
2. C. Amra, *"Light scattering from multilayer optics. Part A: investigation tools"*, J. Opt. Soc. Am. **11**, 197-210 (1994)
3. C. Amra, *"Light scattering from multilayer optics. Part B: application to experiment"*, J. Opt. Soc. Am **11**, 211-226 (1994)